

Autophosphorylation restrains the apoptotic activity of DRP-1 kinase by controlling dimerization and calmodulin binding

Gidi Shani, Sivan Henis-Korenblit,
Ghil Jona, Opher Gileadi,
Miriam Eisenstein¹, Tamar Ziv²,
Arie Admon² and Adi Kimchi³

Departments of Molecular Genetics and ¹Chemical Services, Weizmann Institute of Science, Rehovot 76100 and ²The Smolner Protein Research Center, Department of Biology, Technion Haifa 32000, Israel

³Corresponding author
e-mail: Adi.Kimchi@weizmann.ac.il

DRP-1 is a pro-apoptotic Ca²⁺/calmodulin (CaM)-regulated serine/threonine kinase, recently isolated as a novel member of the DAP-kinase family of proteins. It contains a short extra-catalytic tail required for homodimerization. Here we identify a novel regulatory mechanism that controls its pro-apoptotic functions. It comprises a single autophosphorylation event mapped to Ser308 within the CaM regulatory domain. A negative charge at this site reduces both the binding to CaM and the formation of DRP-1 homodimers. Conversely, the dephosphorylation of Ser308, which takes place in response to activated Fas or tumour necrosis factor- α death receptors, increases the formation of DRP-1 dimers, facilitates the binding to CaM and activates the pro-apoptotic effects of the protein. Thus, the process of enzyme activation is controlled by two unlocking steps that must work in concert, i.e. dephosphorylation, which probably weakens the electrostatic interactions between the CaM regulatory domain and the catalytic cleft, and homodimerization. This mechanism of negative autophosphorylation provides a safety barrier that restrains the killing effects of DRP-1, and a target for efficient activation of the kinase by various apoptotic stimuli.

Keywords: apoptosis/Ca²⁺/calmodulin kinases/DRP-1/negative autophosphorylation

Introduction

Apoptosis is a genetically controlled and evolutionarily conserved cell death process. It plays a role in development, in maintenance of tissue homeostasis and in the cellular response to various damaging insults (Steller, 1995; Jacobson *et al.*, 1997). The list of key players that participate in apoptosis, either negatively or positively, is constantly updated (Ashkenazi and Dixit, 1998; Cryns and Yuan, 1998; Green and Reed, 1998). Recently, a novel family of pro-apoptotic serine/threonine kinases has been identified (Kawai *et al.*, 1999; Inbal *et al.*, 2000). DAP (death-associated protein)-kinase (DAPk), the first described member of this family, is a serine/threonine kinase that is regulated by Ca²⁺/calmodulin (CaM) and is

localized to the actin cytoskeleton. It participates in a wide variety of apoptotic signals including interferon γ , tumour necrosis factor α (TNF- α), Fas and detachment from extracellular matrix (Deiss *et al.*, 1995; Cohen *et al.*, 1997, 1999; Inbal *et al.*, 1997). Four additional kinases that show a significant homology in their catalytic domain to DAPk have recently been identified. ZIP(Dlk)-kinase and DAPk-related protein-1 (DRP-1) are the closest family members, as their catalytic domains share ~80% identity with that of DAPk (Kawai *et al.*, 1998, 1999; Kogel *et al.*, 1998; Inbal *et al.*, 2000). Two more distant DAPk-related proteins are DAPk-related apoptosis-inducing protein kinase 1 (DRAK1) and DRAK2, displaying ~50% identity to DAPk in their kinase domains (Sanjo *et al.*, 1998). ZIP-kinase, DRAK1 and DRAK2 were shown to be nuclear proteins that do not require Ca²⁺/CaM for activation. DRP-1, however, is a cytoplasmic kinase, containing a typical CaM regulatory domain similar to that of DAPk (Inbal *et al.*, 2000). In this sense, DRP-1 is the closest homologue to DAPk, since it also shares a similar mode of activation by calcium.

DRP-1, also named DAPk-2, was cloned based on its homology to the DAPk catalytic domain. As in the case of DAPk, *in vitro* kinase assays confirmed the ability of DRP-1 to phosphorylate an exogenous substrate, myosin light chain (MLC), in a Ca²⁺/CaM-dependent manner. Removal of the CaM regulatory domain converted the enzyme into a constitutively active, Ca²⁺/CaM-independent form. Overexpression of DRP-1 induced cell death, and a dominant-negative DRP-1 mutant protected cells from TNF- α -induced apoptosis, indicating the involvement of DRP-1 in apoptosis (Inbal *et al.*, 2000). The death-promoting effects of DRP-1 depend on the integrity of its catalytic activity, as a catalytically inactive DRP-1 mutant was incapable of inducing apoptosis. The last 40 amino acids comprising the C-terminal tail show no homology to DAPk or to any other known proteins and are required for DRP-1 homodimerization. Interestingly, the death-promoting effects of DRP-1 depended on the presence of this C-terminal tail. Yet, in the absence of the CaM regulatory domain, the C-terminal tail became dispensable in these death assays, an enigma that could not be resolved previously due to the lack of data concerning the precise mode of DRP-1 regulation (Inbal *et al.*, 2000).

All CaM-regulated kinases share a common mechanism of activation of their catalytic domain by Ca²⁺/CaM. The predicted three-dimensional model and the actual crystal structures of a few CaM-regulated kinases gave rise to some hypothetical models of inhibition (Colbran *et al.*, 1989a,b; Kemp *et al.*, 1991; Knighton *et al.*, 1992). According to one model, the CaM regulatory domain, which directly binds activated CaM, displays auto-inhibitory effects by lying within the catalytic cleft, thereby blocking access of substrate. Binding of CaM

induces a conformational change that pulls the auto-inhibitory domain away from the active site, thus permitting subsequent catalysis to occur (Matsushita and Nairn, 1998; Yang and Schulman, 1999).

In addition to the binding of $\text{Ca}^{2+}/\text{CaM}$, most CaM-dependent kinases display additional layer(s) of regulation, largely modulated by phospho-regulatory events. These post-translational modifications confer the fine-tuning regulation of these proteins and are necessary for eliciting the biological responses. Both autophosphorylations and *in trans* phosphorylations have been documented, differing in the position of the target serines/threonines and in their functional effects. For example, CAMKI and CAMKIV require phosphorylation of a unique threonine residue residing within the activation loop of the catalytic domain in order to be activated by $\text{Ca}^{2+}/\text{CaM}$. This important positive phosphorylation occurs *in trans* via another $\text{Ca}^{2+}/\text{CaM}$ -dependent kinase, CAMKK (Haribabu *et al.*, 1995; Watanabe *et al.*, 1996; Matsushita and Nairn, 1998, 1999; Soderling, 1999). In contrast, in the case of CAMKII, an autophosphorylation on Thr286 in the $\text{Ca}^{2+}/\text{CaM}$ regulatory domain renders the kinase partially $\text{Ca}^{2+}/\text{CaM}$ independent. This is a prototypical example of a positive autophosphorylation that serves to relieve the inhibitory effects of this region (Saitoh and Schwartz, 1985; Lai *et al.*, 1986; Miller and Kennedy, 1986; Schworer *et al.*, 1986). In sequential steps, additional autophosphorylations may occur in the absence of $\text{Ca}^{2+}/\text{CaM}$ at either Thr305 or Thr306, both located at the carboxy-proximal part of the $\text{Ca}^{2+}/\text{CaM}$ regulatory domain. These phosphorylations block both rebinding and reactivation by $\text{Ca}^{2+}/\text{CaM}$ (Colbran and Soderling, 1990; Hanson and Schulman, 1992; Colbran, 1993). Thus, the two sequential autophosphorylation events of CaMKII generate a totally $\text{Ca}^{2+}/\text{CaM}$ -independent kinase activity, which may prolong the activation period beyond the point at which intracellular calcium concentrations return to normal levels. Interestingly, autophosphorylation of CaMKII at Thr286 was shown to be required for long-term potentiation and learning capability in mice, further stressing the biological importance of these post-translational modifications (Giese *et al.*, 1998). A positive autophosphorylation within the $\text{Ca}^{2+}/\text{CaM}$ regulatory domain was also documented in smooth muscle MLCK (smMLCK) at Thr803, which converts the catalytic activity into a $\text{Ca}^{2+}/\text{CaM}$ -independent state. Here again, sequential autophosphorylations on Ser815 and Ser823 interfere with the rebinding of CaM (Tokui *et al.*, 1995; Abe *et al.*, 1996).

Being a pro-apoptotic kinase, DRP-1 is expected to be catalytically silent in growing cells and to be activated when necessary in a tightly controlled manner. In this work we specifically addressed the question of whether phospho-regulatory events may dictate the cell-death-promoting effects of DRP-1. Surprisingly, we identified a mechanism of negative autophosphorylation, which is rather unique and novel in the field of CaM-regulated kinases. It was found that in the absence of $\text{Ca}^{2+}/\text{CaM}$, DRP-1 displayed unexpectedly high basal levels of autophosphorylation. The latter was strongly inhibited by $\text{Ca}^{2+}/\text{CaM}$ concentrations that fully activate the enzyme, suggesting inverse relationships between autophosphorylation and substrate phosphorylation. The autophosphoryl-

ation site was mapped to Ser308 in the $\text{Ca}^{2+}/\text{CaM}$ regulatory domain by point mutations and by mass spectrometry. A mutation that mimicked phosphorylation on Ser308 (i.e. substitution to aspartic acid) abrogated the ability of DRP-1 to induce apoptosis, while the reciprocal serine to alanine substitution (which mimics the dephosphorylated state) gave rise to a 'super-killer' mutant. This proved the biological importance of this single negative autophosphorylation, which restrains the apoptotic features of the protein. At the biochemical level, the substitution of Ser308 to aspartic acid decreased the binding affinity to CaM, leading to reduced substrate phosphorylation at limiting CaM concentrations. In parallel, it also inhibited DRP-1 homodimerization. Conversely, mimicking dephosphorylation by the substitution of Ser308 to alanine increased the binding affinity to CaM and elevated the abundance of dimers and higher oligomeric forms of DRP-1. These experiments prove that Ser308 dephosphorylation and DRP-1 dimerization are interconnected and control the CaM responses and enzyme activation. Interestingly, in response to the external apoptotic signals of Fas or TNF- α , DRP-1 autophosphorylation was reduced and dimerization was increased, suggesting that these two interconnected events are targets for regulation. Further analysis of DRP-1 mutants capable of dissecting between phosphorylation and dimerization events, combined with molecular modelling of the catalytic domain, established a novel concept of a safety 'double locking' mechanism for silencing the kinase. It implies that the process of enzyme activation is unique and depends on two unlocking steps. One comprises the relief of the CaM regulatory domain from the catalytic cleft, where it was buried via its negative charge, and the second is the homodimerization process that unexpectedly displays its own positive contribution to CaM binding. Each of these two steps is necessary, yet not sufficient by itself to activate the enzyme. We propose that this unique double locking mechanism evolved in this pro-apoptotic kinase to prevent inappropriate activation, which may be hazardous to cells.

Results

DRP-1 autophosphorylation is inhibited by $\text{Ca}^{2+}/\text{CaM}$ and is inversely correlated with MLC phosphorylation

In search of possible phospho-regulatory events that may affect the death-associated kinase activity of DRP-1, its phosphorylation state was examined *in vitro* under different conditions. To this end, wild-type DRP-1, immunoprecipitated from extracts of transiently transfected 293 cells, was subjected to an *in vitro* kinase assay, using MLC as an exogenous substrate. The assay was performed either in the presence of $\text{Ca}^{2+}/\text{CaM}$ or in their complete absence (the Ca^{2+} chelator EGTA was added instead). The ability of DRP-1 protein to phosphorylate an exogenous substrate (MLC) was highly dependent on the presence of $\text{Ca}^{2+}/\text{CaM}$ (Figure 1A and D). This stood in sharp contrast to the phosphorylation of the DRP-1 protein itself, which was largely inhibited by $\text{Ca}^{2+}/\text{CaM}$ (Figure 1A and C). The latter resulted exclusively from autophosphorylation based on the fact that a catalytically inactive mutant of DRP-1, in which a critical lysine at position 42 was substituted to

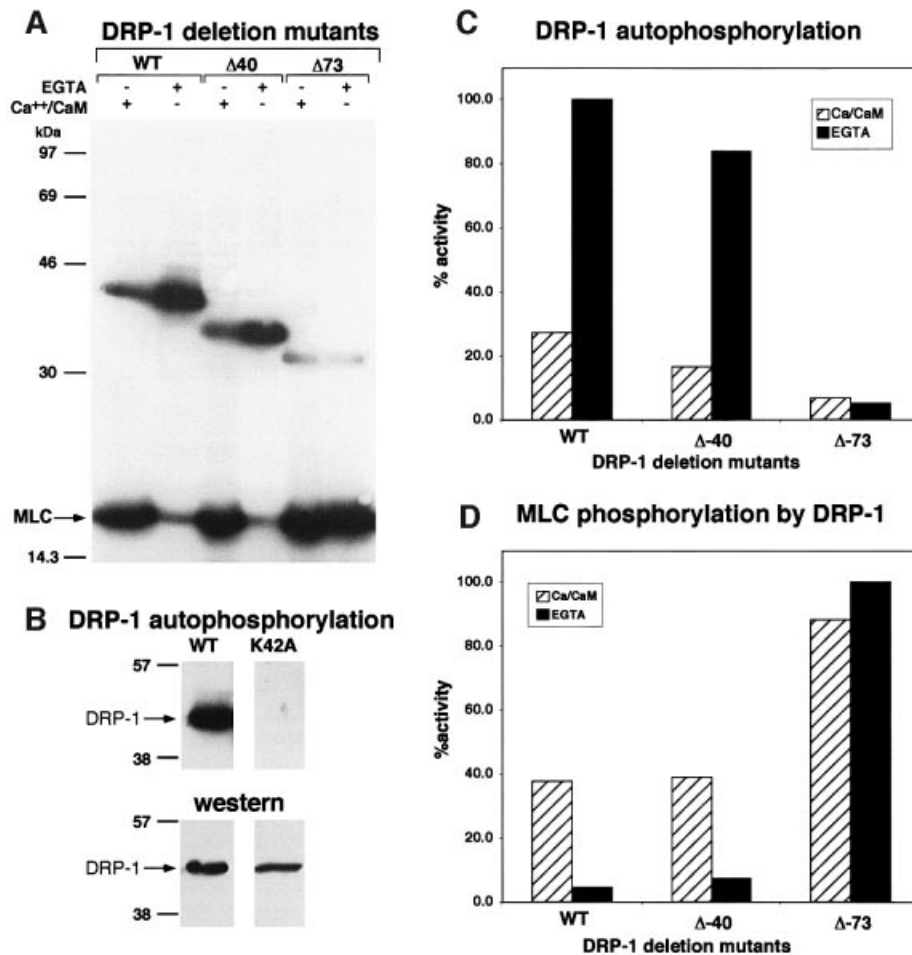


Fig. 1. The *in vitro* kinase activity of DRP-1 is inversely correlated with its autophosphorylation. (A) DRP-1, DRP-1 Δ40 and DRP-1 Δ73 mutant proteins were assayed *in vitro* for kinase activity in the presence of Ca²⁺/CaM or EGTA as described in Materials and methods. Autophosphorylated DRP-1 proteins (between the 30 and 46 kDa markers) and exogenous MLC substrate are shown. (B) The autophosphorylation of wild-type DRP-1 protein is compared with the catalytically inactive K42A mutant (upper part); western blot analysis with anti-FLAG antibodies showing comparable wild-type and mutant protein levels within the immunoprecipitates (lower part). (C and D) Bars showing the relative amount of autophosphorylation and MLC phosphorylation by DRP-1 deletion mutants in the presence or absence of Ca²⁺/CaM, after normalizing to protein expression levels. The latter was determined by incubating the same membranes with anti-HA antibodies followed by ECL detection.

alanine (named K42A), was completely silent in these *in vitro* kinase assays (Figure 1B). Thus, the autophosphorylation activity of DRP-1 in these *in vitro* kinase assays appeared to be inversely correlated with the substrate phosphorylation activity. This prompted us to investigate further the possibility of an auto-inhibitory effect of the DRP-1 autophosphorylated site(s) on its ability to phosphorylate exogenous substrates and to study the relevance of such regulation in the apoptotic process.

Mapping the DRP-1 autophosphorylation site(s) and analysing its relevance in apoptosis

Initially, two C-terminally truncated DRP-1 deletion mutants (DRP-1Δ40 and Δ73 mutants; Figure 2) were used to grossly map the region spanning the autophosphorylated site(s). The exact truncation sites were set according to the homology between DRP-1 and its closely related protein DAPk, and according to the boundaries of the Ca²⁺/CaM regulatory domain in other kinases (Figure 2). Interestingly, while removal of the 40 terminal amino acids of DRP-1 (Δ40 DRP-1) did not interfere with autophosphorylation, removal of 33 additional amino

acids (Δ73 DRP-1), which comprise a Ca²⁺/CaM regulatory domain, abrogated DRP-1 autophosphorylation (Figure 1A and C). Hence, the predominant autophosphorylation site(s) lies within this 33-amino-acid stretch. As expected, the removal of this 33-amino-acid stretch released the kinase from its dependence on Ca²⁺/CaM, enabling MLC phosphorylation even in the presence of the Ca²⁺ chelator EGTA (Figure 1A and D).

Next, we set out to identify the exact autophosphorylation sites. To this end, the CaM regulatory domain of DRP-1 was aligned with CaM regulatory domains of other CaM-binding kinases, including DAPk, smMLCK, CaMKI and CaMKII. This alignment revealed five conserved serine/threonine residues within this region, as tentative autophosphorylation sites (Figure 2). In order to distinguish which of these five candidate residues is the predominant autophosphorylation site, each was systematically substituted to alanine by site-directed mutagenesis, resulting in five new point mutation constructs: S289A, S308A, S310A, S313A and T319A. When tested for kinase activity *in vitro*, four of the mutants, S289A, S310A, S313A and T319A, continued to undergo

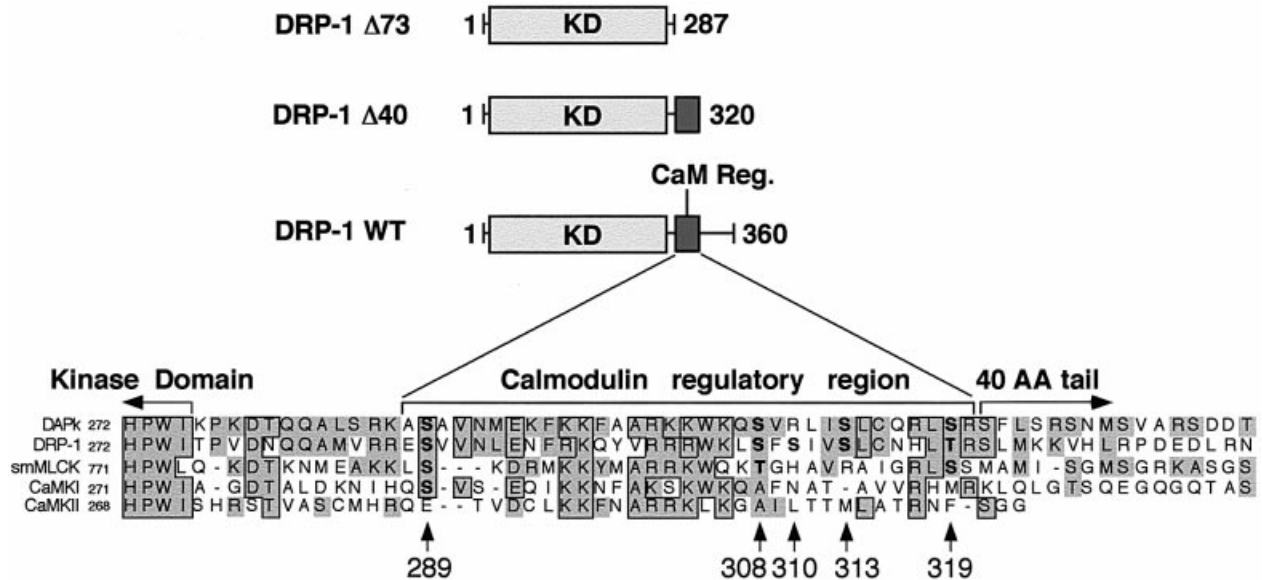


Fig. 2. Deletion map and sequence alignments of the CaM regulatory domain. Schematic representation of DRP-1 deletion mutants and sequence alignments to other related kinases. Multiple sequence alignment of the CaM regulatory (CaM Reg.) and flanking regions of DAPk, DRP-1, smMLCK, CaMKI and CaMKIIa is shown. Identical amino acids are boxed; homologous amino acids are shown in grey. Arrowheads point to candidate phosphorylation sites in the CaM regulatory domain of DRP-1.

autophosphorylation in the absence of $\text{Ca}^{2+}/\text{CaM}$, and, like the wild-type protein, their autophosphorylation was inhibited by $\text{Ca}^{2+}/\text{CaM}$. In contrast, the substitution of Ser308 to alanine abolished the $\text{Ca}^{2+}/\text{CaM}$ -independent autophosphorylation, suggesting that Ser308 is the predominant autophosphorylation site, which is inhibited by $\text{Ca}^{2+}/\text{CaM}$ (Figure 3A and B). These experiments also suggested the existence of a second site (yet minor under the *in vitro* conditions) that is rather subjected to $\text{Ca}^{2+}/\text{CaM}$ -dependent autophosphorylation. The latter was based on the observation that the residual autophosphorylation observed in the presence of $\text{Ca}^{2+}/\text{CaM}$ was still apparent in the S308A mutant, which had lost the $\text{Ca}^{2+}/\text{CaM}$ -independent autophosphorylation (Figure 3A and B).

In parallel to the mutation study, DRP-1 tryptic peptides were analysed by liquid chromatography–mass spectrometry with the intention of identifying the phosphorylation sites by a second independent approach. The analysis was done on the *in vitro* phosphorylated protein that was eluted from the immunoprecipitates after the kinase reaction (the assay was performed in the presence of EGTA under the conditions described in Figures 1A and 3A). The full mass spectrum in Figure 3D identified a peptide whose mass (1021) corresponded to a phosphorylated form of the 305–320 peptide. The collision-induced dissociation (CID) of this peptide further established its identity and was used to determine the exact position of the phosphate. This analysis proved unequivocally that Ser308 was the exclusive site of phosphorylation in this peptide (Figure 3E).

Obviously, the major interest was to test whether the substitution of serine to alanine at position 308 might affect its capability to execute apoptosis *in vivo*. To this aim, the five point mutation constructs were co-transfected into 293 cells together with green fluorescent protein (GFP), as a marker for the transfected cells. Eighteen hours later the percentage of apoptotic cells within the GFP-

positive cell population was scored based on morphological alterations (Inbal *et al.*, 2000). While most of the DRP-1 point mutations gave rise to apoptotic scores similar to that of the wild-type DRP-1 protein (35–45% cell death), introduction of the S308A mutant resulted in a significantly higher apoptotic score (~70%) (Figure 4A). Thus, the prevention of Ser308 phosphorylation, via point mutation, stimulated the apoptotic effects of DRP-1, suggesting that autophosphorylation on this site may negatively affect the death-promoting functions of DRP-1. Mechanistically, the enhanced killing effects could result from stimulation of the catalytic activity, in light of the previously established link between cell death and the enzymatic activity of DRP-1 (Inbal *et al.*, 2000). Yet, when exposed *in vitro* to a large excess of CaM (1 μM), the catalytic activity of the S308A mutant towards MLC did not differ substantially from that of the wild-type protein or of the other mutants (Figure 3A and C). This directed our subsequent research interest into a more detailed and comprehensive biochemical study of the DRP-1 protein, trying to define the precise features that may be regulated by this unique type of negative autophosphorylation on Ser308.

Dephosphorylation of Ser308 enhances oligomerization of DRP-1

Previously we have shown by co-immunoprecipitation assays that DRP-1 undergoes homodimerization, a process that requires the presence of its C-terminal 40-amino-acid tail (Inbal *et al.*, 2000). Consistent with these early observations, when full-length DRP-1 was ectopically expressed and analysed on western blots, a faint band at ~86 kDa, corresponding to the size of a dimer, was detected in addition to the major 42 kDa protein (Figure 4B and C). This indicated that the dimer is quite stable, as traces could still be detected under the denaturing conditions of boiling in the presence of sample buffer.

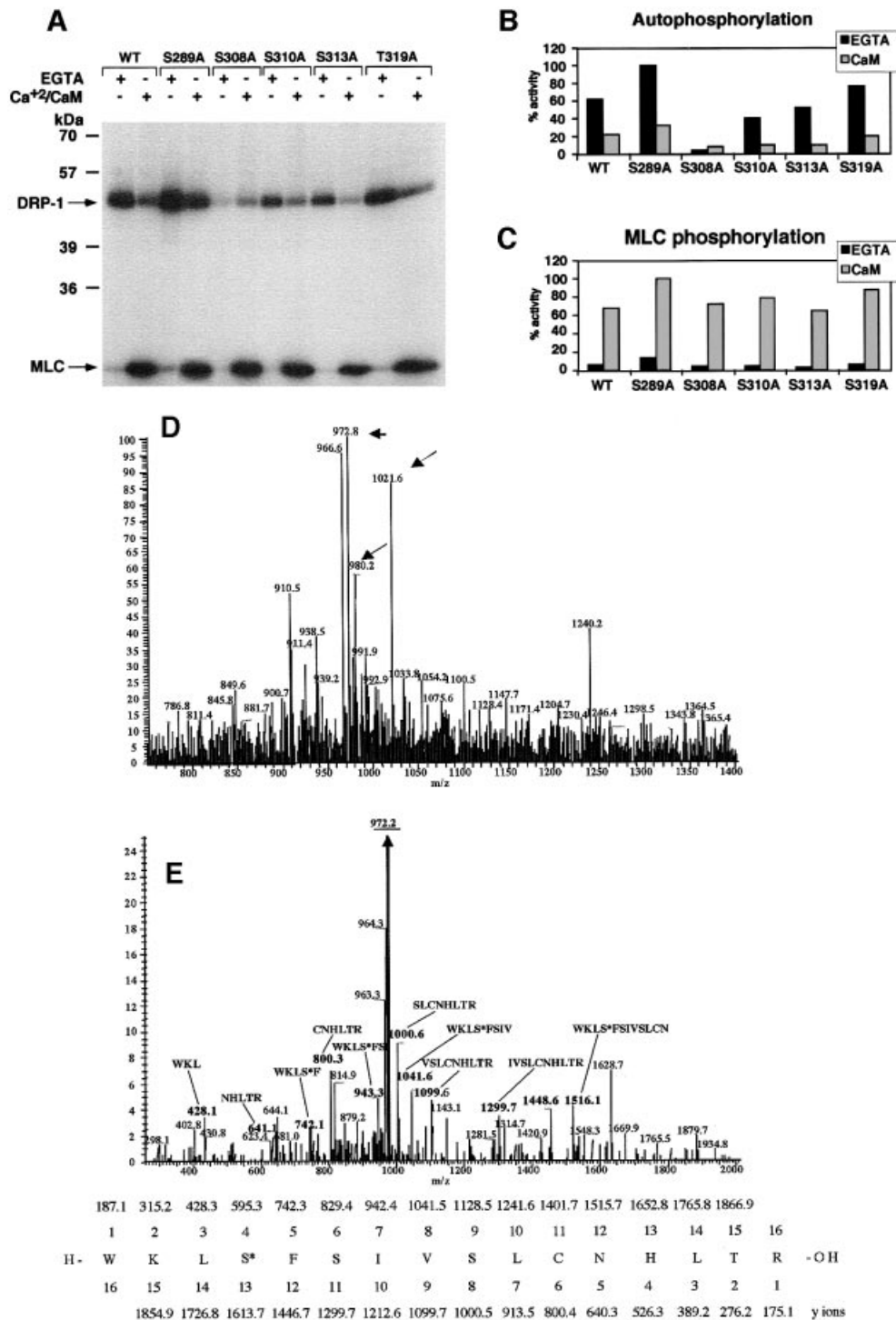


Fig. 3. Identification of Ser308 as the major autophosphorylation site of DRP-1 *in vitro*. (A) DRP-1 and its point mutation constructs were expressed and immunoprecipitated with anti-HA antibodies. The proteins were then assayed *in vitro* for kinase activity (autophosphorylation and MLC phosphorylation) in the presence or absence of Ca²⁺/CaM as described in Figure 1A. (B and C) Bars showing the relative amount of autophosphorylation and MLC phosphorylation by DRP-1 point mutations in the presence or absence of Ca²⁺/CaM, after normalizing to protein expression levels as described in Figure 1C and D. (D and E) Mapping autophosphorylation sites by liquid chromatography–mass spectrometry. (D) Full mass spectrum at retention time 53 min. The masses corresponding to peptide 305–320 in the unphosphorylated ($m/z = 980.2$), the phosphorylated ($m/z = 1021.6$) and the dephosphorylated forms ($m/z = 972.8$) are marked by arrows. (E) Collision-induced dissociation (CID) of the $m/z = 1021.6$ peptide and comparison with the simulated CID of phosphorylated 305–320 DRP-1 peptide. The major fragment $m/z = 972.2$ (underlined) correlates with the doubly charged mass of the full peptide after H₃PO₄ removal (indicating the existence of a single phosphate residue on this peptide). The relevant CID fragments are marked in bold and their amino acid sequence and mass are shown. It indicates that the phosphate residue resides exclusively on Ser308 and not on Ser310, Ser313 or Thr319. The CID simulation of the phosphorylated 305–320 DRP-1 peptide is shown at the bottom. The phosphoserine is marked as S*.

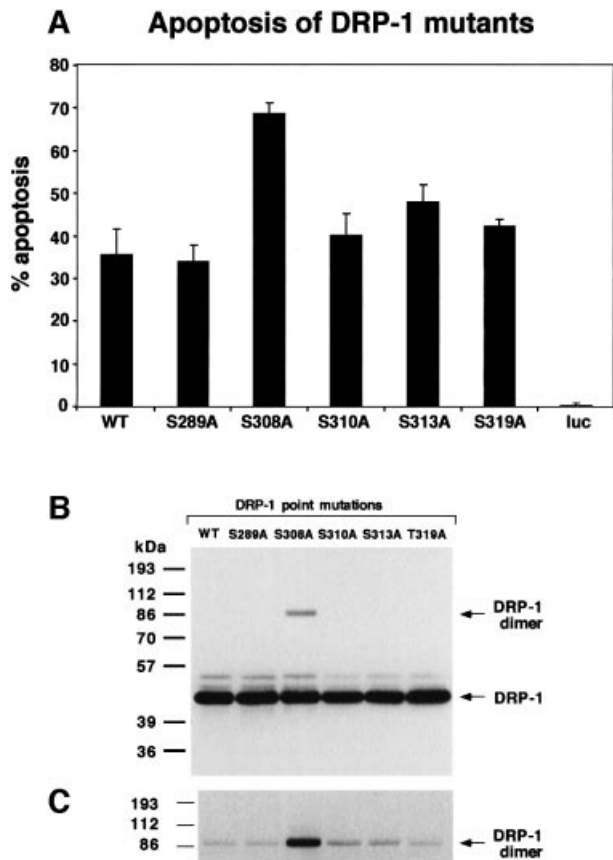


Fig. 4. Substitution of Ser308 to alanine elevates the apoptotic activity and the homodimerization of DRP-1. (A) Percentage of apoptotic cells. Bars showing the percentage of apoptotic cells among the GFP-positive cells resulting from cotransfections of 293 cells with DRP-1 (wild type or point mutations) and GFP. A vector driving the expression of luciferase was used as a non-relevant background control (luc). Quantitation was performed 18 h post-transfection. (B) Protein expression of DRP-1 point mutations in 293 transfected cells. Protein extracts (30 μ g) from the transfected cells shown in (A) were assessed using anti-HA antibodies to visualize the level of DRP-1 protein expression. The positions of DRP-1 monomers and dimers are marked by arrows. (C) Long exposure of the upper part of the blot shown in (B).

Surprisingly, we noticed that the band corresponding to the DRP-1 dimer was substantially enhanced as a result of the S308A point mutation (Figure 4B). In contrast, none of the other four serine to alanine substitutions changed the relative dimer levels substantially (Figure 4C). This raised an interesting possibility that the dephosphorylation of Ser308 may contribute to elevation of DRP-1 dimerization.

The dimerization status of DRP-1 and of the relevant mutants was then directly tested using size fractionation by gel filtration. To this end, we first utilized a Superdex 75 column to separate wild-type, Δ 40 and S308A DRP-1 forms overexpressed in 293 cells, according to their molecular weights. The peak of wild-type DRP-1 eluted in fraction 11, which corresponds to \sim 80 kDa, while the major peak of Δ 40 mutant eluted in fraction 14, which corresponds to \sim 40 kDa (Figure 5). Therefore, it is concluded that while a major portion of wild-type molecules exists in a dimeric form, the Δ 40 mutant, which lacks the C-terminal tail, is mainly a monomer, as

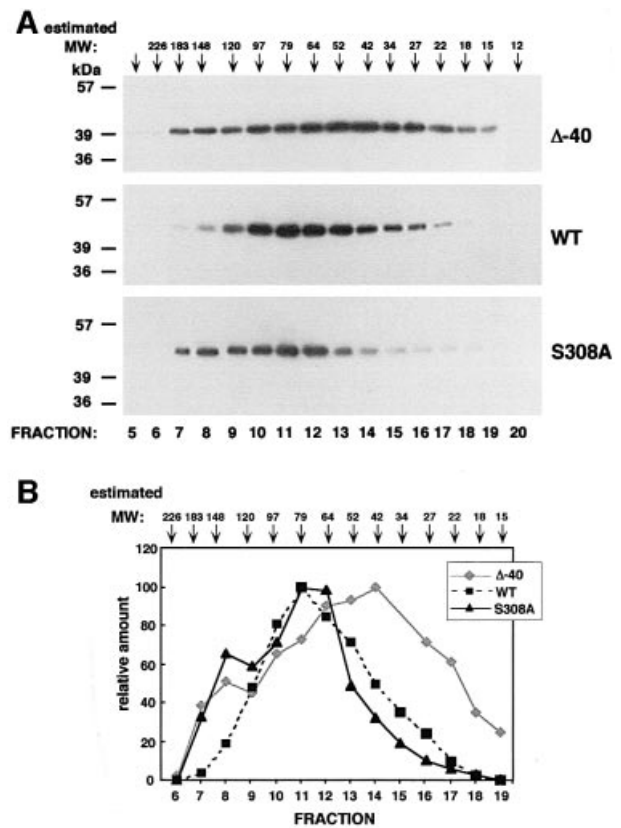


Fig. 5. Analysis of the oligomerization status of DRP-1 mutants by gel filtration. (A) Extracts prepared from cells transfected with Δ 40, wild-type and S308A DRP-1 forms were run on a Superdex 75 column and fractions were analysed by western blotting using anti-HA antibodies. Arrowheads indicate the estimated molecular weights of the various fractions accomplished by running molecular weight markers under the same conditions. (B) A graph showing the relative amount of the various mutants in the different fractions (the peak value in each fractionation is considered as 100%) after densitometric quantitation of the western blot shown in (A).

expected. Interestingly, the elution profile of the S308A point mutant displayed a clear leftward shift towards the higher molecular weight complexes as compared with the wild-type protein (Figure 5). This means that, on the one hand, the serine to alanine substitution reduced the monomeric fraction detected in the wild-type form (fraction 14), and on the other hand, it induced the formation of higher molecular weight forms that are not present in wild-type DRP-1 (fraction 8 in Figure 5). The S308A mutation therefore seemed to increase DRP-1 oligomerization. The precise size of the larger complexes could not be determined in these fractionation profiles since the resolution of the Superdex 75 column is maximal in the range 20–80 kDa and is rather poor at the higher molecular weights. Also, the size of a minor peak, which was detected in the case of Δ 40 mutant at the high molecular weight fraction, could not be determined in these elution profiles for the same reason. In order to improve the fractionation resolution at the higher molecular weight range, the mutant DRP-1 forms were run on a Superose 12 column, whose maximal resolution is in the range 100–200 kDa. Under these conditions, the higher molecular weight forms of the S308A mutant eluted at \sim 150 kDa, which may correspond to a trimer, a tetramer or

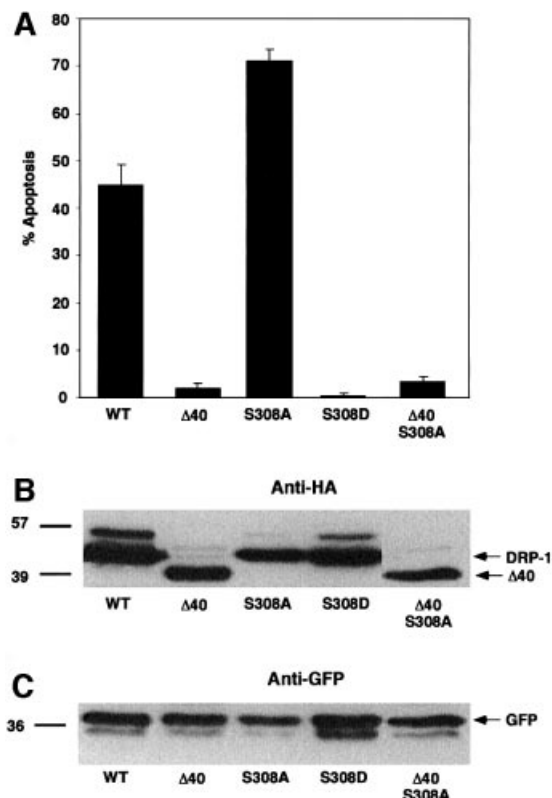


Fig. 6. Induction of apoptosis by DRP-1 mutants; both dephosphorylation at position 308 and homodimerization are necessary conditions. (A) Percentage of apoptotic cells. The bars show the percentage of apoptotic cells resulting from cotransfections of 293 cells with DRP-1 mutants and GFP. Quantitation was performed 22 h post-transfection. This experiment was repeated three times with reproducible results. (B) Protein expression of DRP-1 mutants in 293 transfected cells. Proteins (40 μ g) extracted from the transfected cells were assessed using anti-HA antibodies to visualize the level of expression. (C) The same blot was reacted with anti-GFP antibodies to normalize for the amount of transfected cell lysates in each lane.

other protein complexes (not shown). They clearly differed in their elution profile from the minor population of high molecular weight forms detected in the Δ 40 mutant, whose precise size and nature will be investigated in future experiments.

Negative charge in the critical residue at position 308 abrogates the death-promoting effects of DRP-1

To measure the effect of phosphorylation at position 308 on DRP-1's apoptotic activity, a point mutation that mimics a constantly phosphorylated DRP-1 form was generated by mutating Ser308 to aspartic acid (S308D). This point mutation was previously shown to mimic the phosphorylated state in other proteins, as it imposes a negative charge at the site of interest (Fong and Soderling, 1990; Haribabu *et al.*, 1995; Watanabe *et al.*, 1996). The ability of this 'constitutively phosphorylated' DRP-1 mutant to induce apoptosis was monitored as before and compared with the other DRP-1 mutants (Figure 6A). It was verified that the various DRP-1 forms were expressed at similar levels in these assays by western blotting against a common haemagglutinin (HA) tag (Figure 6B). Furthermore, blotting of the same membrane with anti-

GFP antibodies provided an estimate of the proportion of the transfected cell lysate material in each lane (Figure 6C). Interestingly, the serine to aspartic acid substitution abolished the apoptotic activity (Figure 6A). In fact, the apoptotic scores were even lower than those observed upon transfections with the dimerization-deficient Δ 40 mutant. Thus, an imposed negative charge at position 308 turns off the apoptotic functions of DRP-1 completely, suggesting that dephosphorylation of this serine is necessary for DRP-1-induced apoptosis. Consistent with this conclusion, the reciprocal mutation, S308A, which mimicked the dephosphorylated state, increased the extent of cell death in these experiments (as also shown in Figure 4A). Interestingly, when the serine to alanine substitution was carried out in DRP-1 protein that lacks the C-terminal 40 amino acids (a double mutant named Δ 40 S308A), the apoptotic score was still minimal (Figure 6A). In other words, this point mutation was not capable of overcoming the inability of the Δ 40 mutant to induce apoptosis, suggesting that dimerization is also a necessary condition, and in its absence the dephosphorylation at Ser308 is not sufficient to induce apoptosis.

Dephosphorylation of S308 and homodimerization both increase the binding affinity of DRP-1 to CaM

To test whether the different mutants differ in their CaM sensitivity, a series of kinase assays, using decreasing concentrations of CaM (1 μ M, 100 nM, 10 nM, 1 nM, 0.1 nM and EGTA), were performed with wild-type DRP-1, Δ 40, S308A and S308D mutants (Figure 7A). Interestingly, significant differences in the ability to phosphorylate MLC emerged at the low CaM concentrations. The serine to alanine substitution at position 308 increased the sensitivity of the enzyme to CaM, a feature that could be detected exclusively at low concentrations of CaM (0.1–1 nM). Conversely, the substitution to aspartic acid dramatically reduced the sensitivity to CaM so that even within the range of 10–100 nM CaM, the enzyme was poorly activated (Figure 7A). At a large excess of CaM (1 μ M) the differences were abolished.

When the immunoprecipitates used in Figure 7A were resolved by SDS-polyacrylamide gel fractionations, it was found that the faint band at 86 kDa, which corresponds to traces of the dimeric DRP-1 forms that resist denaturation, was completely abolished in the S308D mutant (in contrast to its increase in the S308A mutant; Figure 7C). To assess more directly the effect of the two mutations at position 308 on the dimerization status of DRP-1, the chemical tool of protein cross-linking with glutaraldehyde was undertaken. The cross-linking agent was added to cell lysates that were prepared from cells transfected with wild-type DRP-1 or with one of the two reciprocal mutants, S308A and S308D. The proteins were thereafter resolved on gels, western blotted and reacted with anti-HA antibodies. It was found that while the S308A DRP-1 mutant migrated exclusively as a dimer, the S308D mutant failed to undergo cross-linking and appeared mainly as a monomer (Figure 7D). Wild-type DRP-1 displayed both forms; the levels of homodimers exceeded the monomeric levels, consistent with the gel size fractionations shown in Figure 5. Thus, the cross-linking experiments provide an independent support that wild-type DRP-1 protein undergoes homodimerization, and specifically show that a

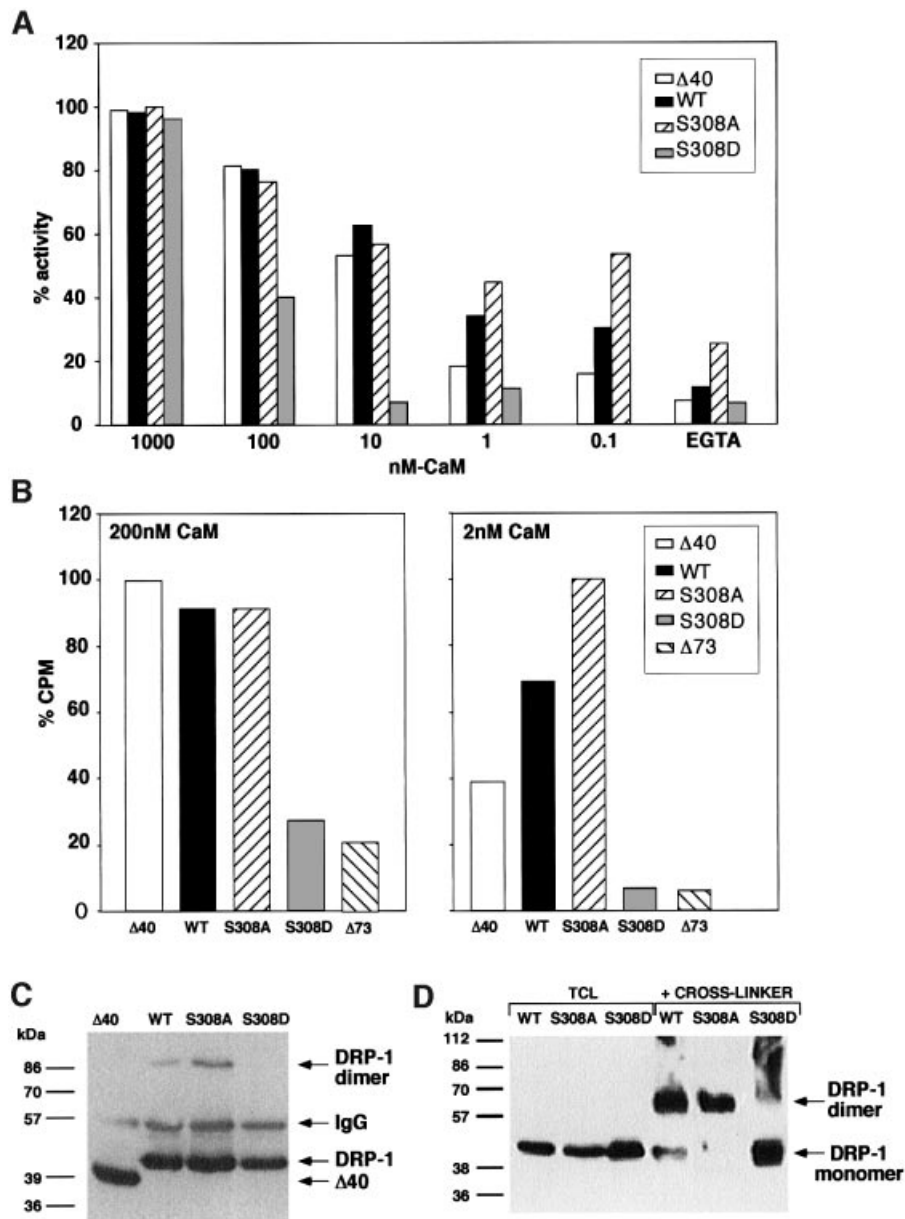


Fig. 7. DRP-1 mutant forms differ in the binding affinity and activation by CaM and in their dimerization status. (A) Differential activation by CaM of DRP-1 mutant forms. $\Delta 40$, wild-type, S308A and S308D DRP-1 constructs were transfected into 293 cells, immunoprecipitated and eluted from the beads with an excess of HA peptide. Equal amounts of the various DRP-1 mutants (estimated by western blotting) were then assayed in an *in vitro* kinase assay towards MLC in the presence of various concentrations of CaM (0–1000 nM). (B) Differential affinity to CaM by DRP-1 mutant forms. $\Delta 40$, wild-type, S308A and S308D DRP-1 constructs were transfected into 293 cells and immunoprecipitated with anti-HA antibodies. Equal amounts of the various DRP-1 mutants were then subjected to CaM binding assay with 200 or 2 nM ^{35}S -labelled CaM as described in Materials and methods. For each CaM concentration the highest binding value was set as 100% (25 227 and 1055 c.p.m. for 200 and 2 nM CaM, respectively); the remaining values were calculated accordingly. (C) The immunoprecipitated beads carrying the various DRP-1 mutants were fractionated on gels and reacted with anti-HA antibodies. The position of DRP-1 monomers and dimers as well as of the immunoglobulin heavy chain is indicated by arrows. (D) Samples of clarified cell extracts (20 μg ; 2 $\mu\text{g}/\mu\text{l}$) were subjected to cross-linking with glutaraldehyde as described in Materials and methods, then separated on gels and western blotted. Another sample from each extract (10 μg) was run in parallel without a prior cross-linking (TCL, total cell lysate). The immunoblots were reacted with anti-HA antibodies. The cross-linked dimer runs faster than predicted due to the globular conformation maintained by the cross-linking agent.

negative charge at position 308 strongly interferes with this process. The question was then whether the negative effect on dimerization may be responsible for the decreased sensitivity to CaM.

It was found that the mere removal of the C-terminal tail (required for dimerization) from the wild-type protein ($\Delta 40$ mutant), also decreased the sensitivity to low concentrations of CaM, thus establishing independently

that lack of dimerization reduced the responses to CaM (Figure 7A). Yet, the effect caused by removal of the tail was much milder when compared with the S308D mutation (it was detected exclusively within the 0.1–1 nM range). This further suggests that the negative charge introduces a second barrier to the catalytic activity, in addition to its inhibitory effects on dimerization, constituting altogether a double locking mechanism.

In parallel to the kinase assays, the binding of the DRP-1 mutants to ^{35}S -labelled CaM was determined directly. The $\Delta 73$ mutant, which lacks the CaM-binding region, served to assess the non-specific background in these binding assays. It was found that the S308D mutant displayed the lowest CaM-binding capability, as detected in both assay conditions performed in the presence of 2 and 200 nM CaM, respectively (Figure 7B). Again, the deletion of the tail had milder consequences, since the $\Delta 40$ mutant displayed a weaker binding activity than the wild-type protein only at low CaM concentrations (2 nM); under these conditions the S308A mutant bound substantially more CaM (Figure 7B). Thus, the pattern of CaM binding to the different mutants was found to correlate with the catalytic activity of these mutants. Together, the assays for CaM sensitivity and CaM binding combined with the cross-linking data of the different mutants suggest that phosphorylation at position 308 reduces the catalytic activity by affecting both the binding affinity to CaM and the status of homodimerization, which by itself contributes to CaM binding.

DRP-1 protein undergoes dephosphorylation *in vivo* upon FAS and TNF- α treatment

It was important to find out first whether Ser308 serves as an autophosphorylation site *in vivo*. To this end, wild-type, S308A and K42A DRP-1 forms, overexpressed in 293 or HFB cells (HeLa cells that stably express the Fas receptors), were labelled *in vivo*. Cells transfected with the above DRP-1 constructs were labelled with [^{33}P]orthophosphate and the ratio of phosphorylation intensity to protein level was calculated. In both cell types S308A showed ~40% reduction in its phosphorylation level compared with the wild type, indicating that S308 serves as a phosphorylation site *in vivo* (Figure 8A and B). The catalytically inactive K42A DRP-1 displayed ~27% of the wild-type phosphorylation level. The latter further implied that while most of the *in vivo* phosphorylation events within the wild-type DRP-1 protein are due to autophosphorylation, a fraction may result from phosphorylation *in trans* by other kinases and may partially contribute to the residual S308A labelling.

Mass spectrometric analysis was then performed again to confirm more directly that Ser308 is also a target for phosphorylation *in vivo*. The tryptic peptide analysis of DRP-1 was carried out right after the immunoprecipitation of the protein from growing HeLa cells as described in Materials and methods. It showed that peptide 307–320 appeared in non-phosphorylated and phosphorylated forms (Figure 8B). The CID analysis of the peptide whose mass corresponded to 835 proved the existence of a single phosphorylation site in this peptide, mapped most likely to Ser308 (Figure 8C).

Next, we asked whether Ser308 is subjected to dephosphorylation in cells as part of DRP-1 activation by apoptotic triggers. To this end, we checked whether activation of TNF- α or Fas receptors leads to any change in the extent of DRP-1 phosphorylation. HFB cells were transfected with wild-type or S308A DRP-1 and incubated for 2 h with [^{33}P]orthophosphate. Subsequently, the cultures were treated for an additional 2 h with agonistic anti-Fas antibodies or with recombinant TNF- α plus cycloheximide. The ratio of phosphorylation intensity to

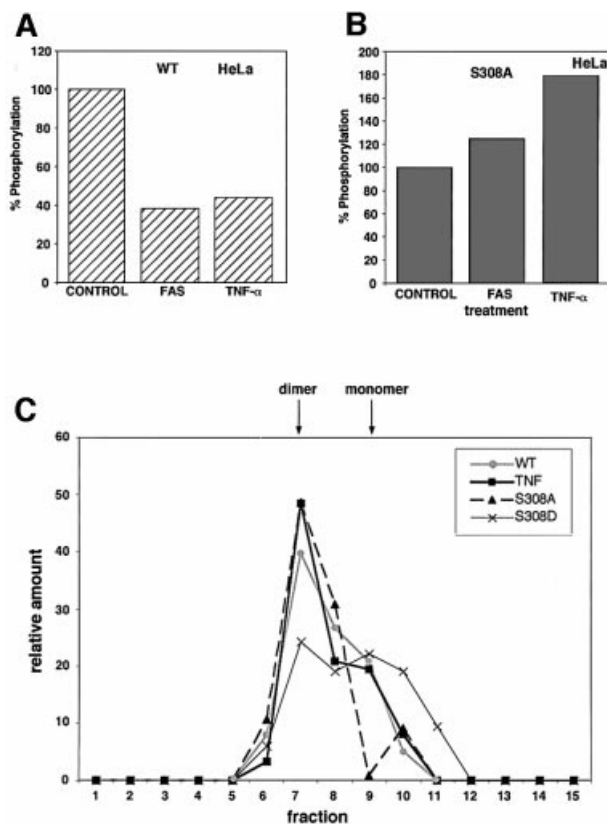


Fig. 9. Ser308 is dephosphorylated *in vivo* in response to activated Fas and TNF- α receptors. (A) HeLa cells ectopically expressing Fas receptors (HFB) were transfected with wild-type DRP-1, *in vivo* labelled and treated with anti-Fas agonistic antibodies or with TNF- α as described in Materials and methods. The levels of ^{33}P incorporated into DRP-1 protein were quantitated in the cell lysates; the values in the untreated culture were set as 100%. (B) The same HeLa cells were transfected with S308A DRP-1, pulse labelled *in vivo*, subjected to activation of Fas or TNF- α receptors, and processed for DRP-1 labelling as in Figure 8B. Again the values in the untreated culture were set as 100%. (C) The different DRP-1 forms (wild type, S308A and S308D) were transfected into HeLa cells; *in vivo*, subjected to transfection with wild-type DRP-1, cells were treated for the last 2.5 h with TNF- α before their extraction. Proteins were separated on a TSK-G3000 column and the pattern of elution was assessed by western blotting with anti-HA antibodies. The densitometric quantitation of the western blots is shown; the relative amounts of DRP-1 protein in each fraction out of the total eluted protein are presented. The positions of the monomer and dimer are indicated by arrows.

protein levels was determined and calculated as described previously. We found that the Fas and TNF- α treatments led to a clear drop in wild-type DRP-1 phosphorylation levels (Figure 9A). In contrast, these treatments did not result in any drop in the residual phosphorylation of S308A DRP-1; on the contrary, an elevation in the intensity of phosphorylation at alternative phosphorylation sites was evident instead (Figure 9B). Therefore, it is concluded that Ser308 undergoes phosphorylation *in vivo*, which is further reduced in response to the apoptotic signals imposed by Fas or TNF- α .

Since the dephosphorylation on 308 was interconnected to DRP-1 homodimerization in our study, the possible effect of TNF- α on the dimerization status was further assessed as a second independent measurement. To this end, cell lysates were fractionated on an HPLC size

exclusion column (TSK-G3000). Extracts were prepared from HFB cells expressing the wild-type DRP-1 form, which were either treated with TNF- α or left untreated. It was found that TNF- α treatment increased the relative levels of dimers (Figure 9C). As a reference, both the S308A and S308D mutants were fractionated in parallel, showing as expected that dimerization (fraction 7) was increased by the alanine mutation and decreased by the substitution to aspartic acid.

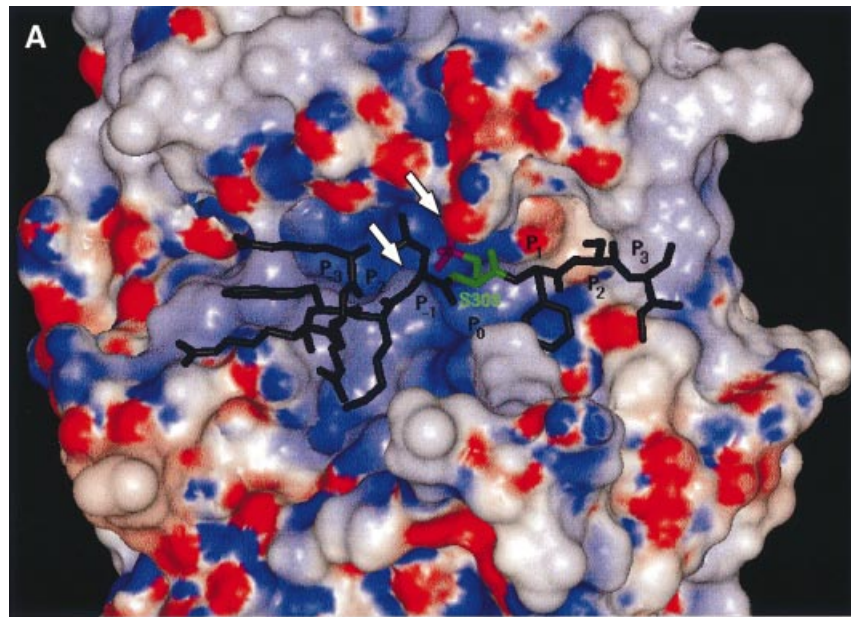
Discussion

Death-promoting kinases need to be tightly controlled in order to prevent inappropriate activation that may have hazardous consequences, on the one hand, and to enable rapid activation in response to the appropriate apoptotic signals, on the other hand. The previous identification of DRP-1 as a Ca²⁺/CaM-regulated kinase suggested that one of its control mechanisms includes the binding to calcium-activated CaM (Kawai *et al.*, 1999; Inbal *et al.*, 2000). This meant that the transient calcium spike arising in response to a variety of apoptotic stimuli could be one of the participants in the process of catalytic activation. Here we report, for the first time, on the identification of an auto-inhibitory phosphorylation event in DRP-1 with critical functional implications. At the cellular level, it restrains the pro-apoptotic features of DRP-1, and becomes a target for regulation when cell death is triggered by external stimuli. At the molecular level, the removal of this negative autophosphorylation must work in concert with DRP-1 homodimerization to elevate the binding affinity to CaM. Thus, phosphorylation at this site introduces a novel type of locking mechanism, previously uncharacterized in the field of CaM-regulated kinases, which prevents inappropriate activation of the catalytic activity at sub-optimal Ca²⁺/CaM concentrations.

The functionally important autophosphorylation site was mapped in this work to Ser308, which resides in the CaM-binding domain of DRP-1. *In vitro* kinase assays demonstrated that this autophosphorylation was inhibited by high concentrations of Ca²⁺-activated CaM. This is consistent with a model in which binding of CaM pulls away the CaM regulatory domain from the catalytic cleft, including, most probably, the region where Ser308 resides (Lou and Schulman, 1989; Kemp *et al.*, 1991; Knighton *et al.*, 1992; Soderling, 1999). Under these conditions of inhibited autophosphorylation, an exogenous substrate was maximally phosphorylated, indicating that Ser308 phosphorylation differs from previously described phosphorylation events in other CaM kinases that were shown to positively regulate substrate phosphorylation. Thus, the concept of negative autophosphorylation was proposed with respect to this site in DRP-1. It was found that substitution of Ser308 to alanine or to aspartic acids, mimicking either constitutively dephosphorylated or phosphorylated states, respectively, significantly affected the ability of DRP-1 to induce apoptosis when ectopically expressed in cells. While imposed dephosphorylation of Ser308 led to a super-killing kinase, imposed phosphorylation abrogated its ability to kill cells completely. Thus, phosphorylation of Ser308 is auto-inhibitory to DRP-1's pro-apoptotic function.

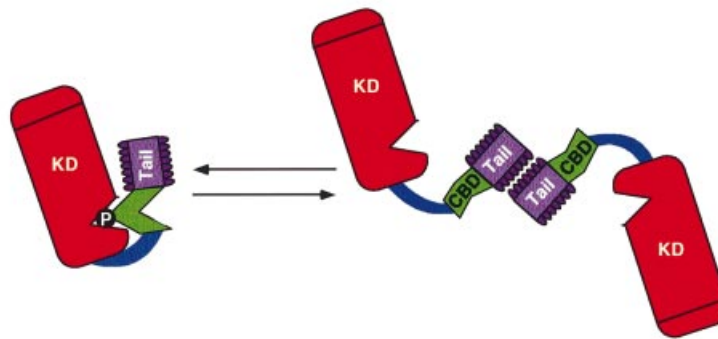
The model structure of the kinase domain of DRP-1 is presented in Figure 10A together with the bound peptide derived from the CaM regulatory domain. It suggests that Ser308 is buried in the kinase active site in the proximity of the ATP-binding loop at a distance that is optimal for the phospho-transfer step. In addition, the active site of the kinase is characterized by a positive charge potential, which can further stabilize the binding of the phosphorylated peptide. As shown in Figure 10A, the peptide binds in the active site with Ser308-PO₃ positioned next to the ATP-binding P-loop, so that the phosphate moiety interacts favourably with this loop and with the positively charged Lys141. Thus, Ser308 phosphorylation might stabilize a 'locked' conformation of the kinase. Locking the catalytic activity by a constitutive phosphorylation, which reduces the accessibility of CaM, is one of the novel layers of regulation, proposed here, which differs from other auto-inhibitory models known in CaM-regulated kinases up to date. The negative charge may also interfere with the interaction of the CaM-binding segment with the CaM molecule as predicted from the model structure of the CaM-binding segment with CaM, which suggests that Ser308 may reside in a hydrophobic pocket of the latter (not shown). Thus, the relief of the phosphorylated CaM-binding segment by CaM should be further weakened considerably by this property as well. The latter possibility was previously described in other kinases, for example, in the case of Thr305 or Thr306 phosphorylation in CaMKII (Colbran and Soderling, 1990; Hanson and Schulman, 1992), there is a basic difference in a sense that in the case of CaMKII, the negative autophosphorylation is not part of a constitutive mechanism that continuously silences the kinase, but it rather terminates a previous CaM-activated signal. In addition, it only corresponds to ~4% of the total Ca²⁺/CaM-dependent autophosphorylation at these sites (Colbran, 1993). Experimentally, the reduced CaM binding was shown here either directly, by measuring the binding of ³⁵S-labelled CaM to the recombinant proteins (Figure 7B), or indirectly, by measuring MLC phosphorylation under rate-limiting CaM concentrations (Figure 7A). The DRP-1 mutants carrying a serine to aspartic acid substitution displayed 100-fold lower affinity to CaM than wild-type protein.

In addition, we studied in this work the regulation of DRP-1 by homodimerization through its C-terminal 40-amino-acid tail. We asked whether homodimerization, like dephosphorylation, also regulates DRP-1 activation, by controlling the CaM responses. First, we established, by size fractionations, that a major portion of the ectopically expressed Δ 40 DRP-1 mutant is indeed in a monomeric 40 kDa state. This contrasted with the wild-type protein, in which the balance between the forms (when over-expressed) was shifted towards dimers. Then, by utilizing direct CaM binding and *in vitro* MLC phosphorylation assays, we found that Δ 40 DRP-1 mutant displayed lower activity than the wild-type protein when exposed to low suboptimal CaM concentrations. Thus, the inability to dimerize properly negatively affected the binding affinity to CaM (see the summary in Figure 10B). This introduces a second, previously uncharacterized layer of regulation, in which the dimerization affects the binding to CaM, by imposing, for example, a conformational change in the



B

DRP-1 ACTIVATION IN APOPTOSIS



	WT	$\Delta 40$	S308A	S308D	$\Delta 40$ S308A
dimerization	+	-	++	+ -	-
Ca ⁺⁺ /CaM binding	++	+	+++	+ -	N.D.
apoptosis	+	-	++	-	-

Fig. 10. (A) Three-dimensional model structure of the kinase domain of DRP-1 with a bound peptide derived from the CaM regulatory segment. The water-accessible surface of the kinase domain is coloured according to the electrostatic potential: red for negative and blue for positive potential. The peptide is shown as a stick diagram with Ser308 emphasized in green and the phosphate moiety in magenta. The arrowheads point to the ATP-binding P-loop and to Lys141. (B) A scheme of DRP-1 structural motifs. The scheme provides a summary of the different features that change by the point mutations or the deletions including the dimerization, CaM-binding and apoptotic functions. The various domains are marked by KD (kinase domain), CBD (CaM-binding domain) and Tail (the C-terminal 40-amino-acid peptide). The catalytic cleft is marked by a V-shaped structure in which the phosphate residue on Ser308 resides. N.D., not done.

CaM regulatory segment that facilitates the interactions with the CaM molecule.

Another unexpected twist in these studies emerged once we found that the S308A mutation actually enhanced the conversion of DRP-1 protein into higher oligomeric forms. This further suggested that these two parameters are biochemically linked to each other and that the phosphorylation at position 308 may prevent the appropriate exposure of the dimerization domains for interaction with

each other (see a tentative model in the scheme in Figure 10B). Overall, a simple interpretation would be that dephosphorylation and homodimerization are sequential steps of a single activation pathway, i.e. the contribution of dephosphorylation to CaM binding takes place exclusively through its effects on dimerization. Yet, once we increased the resolution of our biochemical analysis using a set of DRP-1 mutants, it was clear that the negative charge has an additional, dimerization-independent effect on CaM

binding, raising the double locking concept, which is based on two cooperative events. It was found that although S308D substitution and the tail deletion mutant each prevented dimerization, the former had a much more dramatic effect on the binding affinity to CaM (Figure 10B). This means that inhibition of dimerization and its associated effects on CaM binding are not sufficient by themselves to get maximal effects. The electrostatic interactions that bury the CaM regulatory segment in the catalytic cleft, as previously discussed (Figure 10A), must work in concert to provide an efficient double locking mechanism. Consistently, cooperative interactions are also required for the unlocking process. Thus, the S308A 'activating mutation' was not effective in apoptosis in the absence of the C-terminal tail, suggesting that removal of negative charge is not sufficient by itself, and emphasizing the necessity of dimerization for apoptotic activation. Additionally, we found that another mutation, S308E, which still retained its capability to dimerize, displayed a reduced CaM-binding affinity (data not shown), suggesting that dimerization is also not sufficient by itself to unlock the catalytic activity as long as some negative charge is still present at position 308. Thus, the interconnected dephosphorylation and dimerization events must cooperate to unlock the catalytic activity.

Upon triggering of death signalling by anti-Fas agonistic antibodies or by the addition of TNF- α , the restraints imposed by the negative autophosphorylation are removed. This is achieved by Ser308 dephosphorylation, probably via a specific as yet unidentified phosphatase. It results in a protein that displays increased tendency to dimerize and that according to our biochemical analysis should be much more sensitive to activation by Ca²⁺/CaM. Elevated sensitivity to CaM may facilitate 'sensing' of the Ca²⁺ spike, which usually accompanies an apoptotic signal, for example, by widening the window of DRP-1 activation beyond the time where intracellular Ca²⁺ concentrations are maximal. Alternatively, it may serve as a bypass mechanism that enables DRP-1 activation at basal Ca²⁺ levels. Thus, the dephosphorylation of Ser308 seems to be a major target for DRP-1 activation during apoptosis.

Finally, it should be mentioned that additional sites on DRP-1 undergo phosphorylation, in correlation with the activated form of DRP-1 kinase. These phosphorylation events can be detected *in vitro* in the presence of Ca²⁺/CaM, although to a much lesser extent than Ser308 autophosphorylation. Death-associated phosphorylations on residues other than Ser308 that are enhanced by treatment with Fas and TNF- α have also been detected *in vivo*, when the S308A-activated mutant was compared with the wild-type protein. Further research should be invested in order to elucidate these sites and their functional implications.

Materials and methods

DNA constructs

Wild-type, K42A and deletion mutants of DRP-1 were expressed from pcDNA3-HA vector as previously described (Inbal *et al.*, 2000). Point mutations were introduced in wild-type DRP-1-containing plasmid, by the QuikChange™ Site-Directed Mutagenesis Kit (Stratagene), using a set of primers encompassing the inserted point mutations, to generate

S308A, S308D and S308E. DRP-1 K42A-FLAG was generated as previously described (Inbal *et al.*, 2000).

Cell lines, transfections and apoptotic assays

293 embryonic kidney or HFB cells were grown in Dulbecco's modified Eagle's medium (Biological Industries) supplemented with 10% fetal calf serum (Bio-Lab). For transient transfection, 1×10^5 , 1×10^6 or 4.5×10^6 cells were seeded on 6-well, 9 cm or 15 cm plates, respectively, 1 day prior to transfection. Transfections were carried out using the calcium phosphate method for 293 cells, or with Superfect transfection reagent (Qiagen) according to the manufacturer's instructions, in HFB cells. For cell death assays, a mixture containing 2 μ g (Figure 4) or 5 μ g (Figure 7) of cell-death-inducing plasmids (pcDNA3 expressing the different DRP-1 constructs) and 0.5 μ g of pEGFP-N1 plasmid (Clontech) was used. For each transfection, three fields, each consisting of at least 100 GFP-positive cells, were scored for apoptotic cells according to their morphology. At the indicated time point cell lysates were prepared from the transient transfections for protein analysis.

Cell lysates and immunoprecipitations

Cells were washed with phosphate-buffered saline and lysed in cold B-buffer [100 mM KCl, 0.5 mM EDTA, 20 mM HEPES-KOH pH 7.6, 0.4% NP-40, 20% glycerol, 1 mM dithiothreitol (DTT)], protease inhibitors: 4 μ g/ml aprotinin, 5 μ g/ml pepstatin A, 5 μ g/ml leupeptin, 1 mM phenylmethylsulfonyl fluoride, and phosphatase inhibitors: 1 mM NaF, 10–50 mM β -glycerol phosphate and 200 nM okadaic acid when indicated (Figure 9C). A second extraction buffer used was PLB (10 mM NaH₂PO₄ pH 7.5, 100 mM NaCl, 1% Triton X-100, 0.1% SDS, 0.5% sodium deoxycholate and 5 mM EDTA) supplemented with protease and phosphatase inhibitors. For immunoprecipitation experiments, 1 mg of protein extract was pre-cleared by protein G-PLUS-Agarose beads (Santa Cruz Biotechnology) for 2 h at 4°C. The pre-cleared extracts were incubated with the beads and with 20 μ l of anti-HA monoclonal antibodies (16B12; BabCO) for 2 h at 4°C. Immunoprecipitates were washed repeatedly three times with B-buffer or PLB and twice with kinase buffer. Where indicated, the proteins were eluted by addition of 50 μ l of HA peptide (500 ng/ μ l) (BabCO).

In vitro kinase assay

293 cells were transfected with various HA-tagged DRP-1 constructs, immunoprecipitated as described above and washed with kinase reaction buffer (50 mM HEPES pH 7.5, 20 mM MgCl₂ and 0.1 mg/ml bovine serum albumin). The proteins bound to the beads were incubated for 9 min (Figure 1) or 5 min (Figure 3) at 30°C in 50 μ l of reaction buffer containing 15 μ Ci of [γ -³²P]ATP (3 pmol), 50 μ M ATP, 4 μ g of chicken gizzard MLC (Sigma), and either 1 μ M bovine CaM (Sigma) and 0.5 mM CaCl₂, or 4 mM EGTA. Protein sample buffer was added to terminate the reaction, and after boiling, the proteins were analysed on 11% SDS-PAGE. The gel was blotted onto a nitrocellulose membrane and ³²P-labelled proteins were visualized by autoradiography and quantified by PhosphorImager densitometric analysis.

Mass spectrometric analysis

Cell cultures (4.5×10^6 cells per 15 cm plates) were transfected with wild-type DRP-1 (40 μ g into 293 cells and 1.5 μ g into HeLa cells for the experiments described in Figures 3D and 8B, respectively). Cell extracts were prepared 22 h post-transfection and the ectopically expressed DRP-1 was immunoprecipitated with anti-FLAG antibodies coupled to agarose beads (M2 affinity gel; Sigma). In the experiment described in Figure 3D, the immunoprecipitated protein was subjected to *in vitro* kinase assay in the presence of EGTA, as described above. Subsequently, DRP-1 protein was eluted from the Sepharose beads by adding an excess of FLAG peptide (incubation with 1 mg/ml peptide for 1 min at 25°C). The eluted protein was subjected to reduction with 10 mM DTT, modification with 100 mM iodoacetamide in 10 mM ammonium bicarbonate, and trypsinization with 100 nM ammonium bicarbonate containing ~1 μ g of trypsin per sample. In the experiment described in Figure 8B, the immunoprecipitated protein was immediately separated by SDS-PAGE followed by Coomassie Blue staining and in gel proteolysis. The stained protein bands in the gel were cut with a clean razor blade and the proteins in the gel were reduced with 10 mM DTT and modified with 100 mM iodoacetamide in 10 mM ammonium bicarbonate. The gel pieces were treated with 50% acetonitrile in 10 mM ammonium bicarbonate to remove the stain from the proteins followed by drying the gel pieces. The dried gel pieces were rehydrated with 10 mM ammonium bicarbonate containing ~1 μ g of trypsin per sample. The gel pieces were incubated overnight at 37°C and the resulting peptides were recovered with 60%

acetonitrile with 0.1% trifluoroacetate. The tryptic peptides were resolved by reverse-phase chromatography on 0.075 × 300 mm fused silica capillaries (New Objective, PicoTip) home-filled with porous R2 (Perseptive). The peptides were separated by an 80 min linear gradient of 5–95% acetonitrile in 0.1% acetic acid at a flow rate of ~1 µl/min. The liquid from the column was electrosprayed into an ion-trap mass spectrometer (LCQ, Finnigan, San Jose, CA). Mass spectrometry was performed in the positive ion mode using a repetitively full mass spectrometry scan followed by CID of the potential DRP-1 peptides. The mass spectrometry data were compared with simulated proteolysis and CID of the DRP-1 protein using the Sequest software (J.Eng and J.Yates, University of Washington and Finnigan, San Jose).

Analysis of DRP-1 by gel filtration

293 cells (4.5×10^6) were plated on 15 cm plates and transfected with 40 µg of DNA from the specified constructs. At 22 h post-transfection, cells were collected and proteins were extracted using B-buffer supplemented with protease and phosphatase inhibitors (Sigma) at 4°C. The extracts were then sonicated to break nucleic acids, and spun for 20 min at 13 000 g to remove insoluble material. Four milligrams of each sample were run on either Superdex 75 or Superose 12 gel-filtration columns (Pharmacia), previously equilibrated with running-buffer (20 mM HEPES pH 7.5, 20 mM MgCl₂, 50 mM KCl and 10% glycerol) supplemented with protease and phosphatase inhibitors (Sigma) at 4°C. The columns were run at 0.25 ml/min, collecting 0.4 ml fractions. Analysis of the various fractions was carried out using anti-HA western blot analysis as described above. For determining molecular weight sizes the following markers (Sigma) were run in the same conditions on both columns: dextran blue, β-amylase, alcohol dehydrogenase, bovine serum albumin and carbonic anhydrase, at 2000, 200, 150, 66 and 29 kDa, respectively.

Analysis of DRP-1 by size exclusion HPLC

HeLa cells (4.5×10^6) were plated on 15 cm plates and transfected with 9 µg of DNA from each of the specified constructs (wild type, S308A, S308D). At 15.5 h post-transfection, the cells that were transfected with wild-type DRP-1 were either treated with a combination of cycloheximide (CHX, 10 µg/ml; Sigma) and TNF-α (50 ng/ml; R&D systems Inc.), or left untreated. At 18 h post-transfection, cells were collected and proteins were extracted using B-buffer supplemented with protease and phosphatase inhibitors (Sigma) at 4°C. The extracts were then sonicated and cleared by centrifugation for 1 h at 100 000 g. Each extract sample (2.25 mg) was run on a TSK-G3000-SW column (TosoHaas), previously equilibrated with running-buffer (50 mM phosphate buffer pH 7.0, 150 mM NaCl and 10 mM β-glycerol phosphate). The column was run at 1 ml/min, collecting 1 ml fractions. Analysis of the various fractions was carried out using anti-HA western blot analysis as described above. For determining molecular weight sizes the following markers (Sigma) were run in parallel: dextran blue, β-amylase, alcohol dehydrogenase, bovine serum albumin and carbonic anhydrase, at 2000, 200, 150, 66 and 29 kDa, respectively.

CaM-binding assay

293 cells were transfected with various HA-tagged DRP-1 mutants (40 µg of DNA). Proteins were extracted in B-buffer and immunoprecipitated as indicated above. 1/25 or 1/9 of the total immunoprecipitated protein was incubated for 1.5 h at 30°C with 200 or 2 nM of recombinant ³⁵S-labelled CaM in CaM-binding buffer (50 mM Tris pH 7.5, 150 mM NaCl and 1 mM CaCl₂), respectively. The proteins were washed five times (5 min each) in CaM-binding buffer, and 1 ml of scintillation fluid (Ultima gold, Packard) was added to each point. The bound radioactivity was detected using a standard β-counter.

Cross-linking assays

293 cells were transfected with wild type, S308A or S308D mutants of DRP-1 (a mixture of 3.5 µg of HA-tagged protein plus 3.5 µg of FLAG-tagged protein per 15 cm plate). After 18 h, proteins were extracted in B-buffer (without DTT) and extracts were cleared by centrifugation at 100 000 g for 1 h at 4°C. Glutaraldehyde (Sigma) at a final concentration of 0.25% was added to each extract (20 µg; 2 µg/µl) for 15 min at 4°C and the reaction was stopped by addition of sodium borohydride (at a final concentration of 0.2%). After 20 min, the proteins were resolved on gels and western blotted with anti-HA antibodies.

Metabolic labelling of proteins

293 or HFB cells were transfected with DRP-1 mutants as indicated. Twelve hours post-transfection the medium was changed to orthophos-

phate-depleted medium supplemented with 100 µCi/ml ³³P-labelled orthophosphate (Amersham), and the cells were harvested after 12 h. The proteins were extracted, immunoprecipitated and fractionated on SDS-PAGE, as indicated above. The labelling of DRP-1 proteins was determined by dividing the phosphorylation rate (assessed by densitometry via a PhosphorImager) to the relative amount of protein (assessed by western blotting). When exposed to cytokines, HFB cells were treated with a combination of CHX (10 µg/ml; Sigma) and TNF-α (50 ng/ml; R&D systems Inc.), or a combination of protein A (5 µg/ml; Sigma) and anti-Fas agonistic antibodies (100 ng/ml IgG3), at 2 h after addition of 100 µCi/ml ³³P-labelled orthophosphate. After two additional hours the cells were harvested and protein phosphorylation was assessed as indicated above.

Molecular modelling

A three-dimensional model structure of the kinase domain of DRP-1 was constructed based on the X-ray structure of phosphorylase kinase in complex with a peptide substrate (Lowe *et al.*, 1997) (Protein Data Bank code 2phk). The characteristically conserved residues in the kinase domain were easily identified and used to verify the psi-blast sequence alignment (Altschul *et al.*, 1997). Hence, despite the low sequence identity (38%) a reliable model could be built. The model was constructed using the Homology module of MSI (MSI, San Diego, CA). It was verified by calculating the 3D-1D self-compatibility score (Luthy *et al.*, 1992), which was 102.2 (the expected score for a protein of this length is 118.6). The electrostatic potential around the molecule was calculated using the program Delphi (Gilson and Honig, 1988), with the PARSE set of charges and atomic radii (Sitkoff *et al.*, 1994). The binding of the peptide to the DRP-1 kinase domain was modelled in analogy to the binding of the peptide substrate to phosphorylase kinase.

Acknowledgements

We thank Dr Daniel Tal for his devoted help and advice on the HPLC fractionations, and Dr Menachem Rubinstein for advice on the cross-linking experiments. We thank P.Krammer for providing the anti-Fas agonistic antibodies and Shani Bialik for reading the manuscript. This work was supported in part by the Feinberg Foundation and by a grant from DIP (Deutsch-Israelische Projektkooperation). A.K. is the incumbent of the Helena Rubinstein Chair of Cancer Research.

References

- Abe,M., Hasegawa,K. and Hosoya,H. (1996) Activation of chicken gizzard myosin light chain kinase by Ca²⁺/calmodulin is inhibited by autophosphorylation. *Cell Struct. Funct.*, **21**, 183–188.
- Altschul,S.F., Madden,T.L., Schaffer,A.A., Zhang,J., Zhang,Z., Miller,W. and Lipman,D.J. (1997) Gapped BLAST and PSI-BLAST: a new generation of protein database search programs. *Nucleic Acids Res.*, **25**, 3389–3402.
- Ashkenazi,A. and Dixit,V.M. (1998) Death receptors: signaling and modulation. *Science*, **281**, 1305–1308.
- Cohen,O., Feinstein,E. and Kimchi,A. (1997) DAP-kinase is a Ca²⁺/calmodulin-dependent, cytoskeletal-associated protein kinase, with cell death-inducing functions that depend on its catalytic activity. *EMBO J.*, **16**, 998–1008.
- Cohen,O., Inbal,B., Kissil,J.L., Raveh,T., Berissi,H., Spivak-Kroizaman,T., Feinstein,E. and Kimchi,A. (1999) DAP-kinase participates in TNF-α- and Fas-induced apoptosis and its function requires the death domain. *J. Cell Biol.*, **146**, 141–148.
- Colbran,R.J. (1993) Inactivation of Ca²⁺/calmodulin-dependent protein kinase II by basal autophosphorylation. *J. Biol. Chem.*, **268**, 7163–7170.
- Colbran,R.J. and Soderling,T.R. (1990) Calcium/calmodulin-independent autophosphorylation sites of calcium/calmodulin-dependent protein kinase II. Studies on the effect of phosphorylation of threonine 305/306 and serine 314 on calmodulin binding using synthetic peptides. *J. Biol. Chem.*, **265**, 11213–11219.
- Colbran,R.J., Schworer,C.M., Hashimoto,Y., Fong,Y.L., Rich,D.P., Smith,M.K. and Soderling,T.R. (1989a) Calcium/calmodulin-dependent protein kinase II. *Biochem. J.*, **258**, 313–325.
- Colbran,R.J., Smith,M.K., Schworer,C.M., Fong,Y.L. and Soderling,T.R. (1989b) Regulatory domain of calcium/calmodulin-dependent protein kinase II. Mechanism of inhibition and regulation by phosphorylation. *J. Biol. Chem.*, **264**, 4800–4804.

- Cryns, V. and Yuan, J. (1998) Proteases to die for. *Genes Dev.*, **12**, 1551–1570.
- Deiss, L.P., Feinstein, E., Berissi, H., Cohen, O. and Kimchi, A. (1995) Identification of a novel serine/threonine kinase and a novel 15-kD protein as potential mediators of the γ interferon-induced cell death. *Genes Dev.*, **9**, 15–30.
- Fong, Y.L. and Soderling, T.R. (1990) Studies on the regulatory domain of Ca^{2+} /calmodulin-dependent protein kinase II. Functional analyses of arginine 283 using synthetic inhibitory peptides and site-directed mutagenesis of the α subunit. *J. Biol. Chem.*, **265**, 11091–11097.
- Giese, K.P., Fedorov, N.B., Filipkowski, R.K. and Silva, A.J. (1998) Autophosphorylation at Thr286 of the α calcium-calmodulin kinase II in LTP and learning. *Science*, **279**, 870–873.
- Gilson, M.K. and Honig, B. (1988) Calculation of the total electrostatic energy of a macromolecular system: solvation energies, binding energies and conformational analysis. *Proteins*, **4**, 7–18.
- Green, D.R. and Reed, J.C. (1998) Mitochondria and apoptosis. *Science*, **281**, 1309–1312.
- Hanson, P.I. and Schulman, H. (1992) Inhibitory autophosphorylation of multifunctional Ca^{2+} /calmodulin-dependent protein kinase analyzed by site-directed mutagenesis. *J. Biol. Chem.*, **267**, 17216–17224.
- Haribabu, B., Hook, S.S., Selbert, M.A., Goldstein, E.G., Tomhave, E.D., Edelman, A.M., Snyderman, R. and Means, A.R. (1995) Human calcium-calmodulin dependent protein kinase I: cDNA cloning, domain structure and activation by phosphorylation at threonine-177 by calcium-calmodulin dependent protein kinase I kinase. *EMBO J.*, **14**, 3679–3686.
- Inbal, B., Cohen, O., Polak-Charcon, S., Kopolovic, J., Vadai, E., Eisenbach, L. and Kimchi, A. (1997) DAP kinase links the control of apoptosis to metastasis. *Nature*, **390**, 180–184.
- Inbal, B., Shani, G., Cohen, O., Kissil, J.L. and Kimchi, A. (2000) Death-associated protein kinase-related protein 1, a novel serine/threonine kinase involved in apoptosis. *Mol. Cell. Biol.*, **20**, 1044–1054.
- Jacobson, M.D., Weil, M. and Raff, M.C. (1997) Programmed cell death in animal development. *Cell*, **88**, 347–354.
- Kawai, T., Matsumoto, M., Takeda, K., Sanjo, H. and Akira, S. (1998) ZIP kinase, a novel serine/threonine kinase which mediates apoptosis. *Mol. Cell. Biol.*, **18**, 1642–1651.
- Kawai, T., Nomura, F., Hoshino, K., Copeland, N.G., Gilbert, D.J., Jenkins, N.A. and Akira, S. (1999) Death-associated protein kinase 2 is a new calcium/calmodulin-dependent protein kinase that signals apoptosis through its catalytic activity. *Oncogene*, **18**, 3471–3480.
- Kemp, B.E., Pearson, R.B. and House, C.M. (1991) Pseudosubstrate-based peptide inhibitors. *Methods Enzymol.*, **201**, 287–304.
- Knighton, D.R., Pearson, R.B., Sowadski, J.M., Means, A.R., Ten Eyck, L.F., Taylor, S.S. and Kemp, B.E. (1992) Structural basis of the intrasteric regulation of myosin light chain kinases. *Science*, **258**, 130–135.
- Kogel, D., Plottner, O., Landsberg, G., Christian, S. and Scheidtmann, K.H. (1998) Cloning and characterization of Dlk, a novel serine/threonine kinase that is tightly associated with chromatin and phosphorylates core histones. *Oncogene*, **17**, 2645–2654.
- Lai, Y., Nairn, A.C. and Greengard, P. (1986) Autophosphorylation reversibly regulates the Ca^{2+} /calmodulin-dependence of Ca^{2+} /calmodulin-dependent protein kinase II. *Proc. Natl Acad. Sci. USA*, **83**, 4253–4257.
- Lou, L.L. and Schulman, H. (1989) Distinct autophosphorylation sites sequentially produce autonomy and inhibition of the multifunctional Ca^{2+} /calmodulin-dependent protein kinase. *J. Neurosci.*, **9**, 2020–2032.
- Lowe, E.D., Noble, M.E., Skamnaki, V.T., Oikonomakos, N.G., Owen, D.J. and Johnson, L.N. (1997) The crystal structure of a phosphorylase kinase peptide substrate complex: kinase substrate recognition. *EMBO J.*, **16**, 6646–6658.
- Luthy, R., Bowie, J.U. and Eisenberg, D. (1992) Assessment of protein models with three-dimensional profiles. *Nature*, **356**, 83–85.
- Matsushita, M. and Nairn, A.C. (1998) Characterization of the mechanism of regulation of Ca^{2+} /calmodulin-dependent protein kinase I by calmodulin and by Ca^{2+} /calmodulin-dependent protein kinase kinase. *J. Biol. Chem.*, **273**, 21473–21481.
- Matsushita, M. and Nairn, A.C. (1999) Inhibition of the Ca^{2+} /calmodulin-dependent protein kinase I cascade by cAMP-dependent protein kinase. *J. Biol. Chem.*, **274**, 10086–10093.
- Miller, S.G. and Kennedy, M.B. (1986) Regulation of brain type II Ca^{2+} /calmodulin-dependent protein kinase by autophosphorylation: a Ca^{2+} -triggered molecular switch. *Cell*, **44**, 861–870.
- Saitoh, T. and Schwartz, J.H. (1985) Phosphorylation-dependent subcellular translocation of a Ca^{2+} /calmodulin-dependent protein kinase produces an autonomous enzyme in Aplysia neurons. *J. Cell Biol.*, **100**, 835–842.
- Sanjo, H., Kawai, T. and Akira, S. (1998) DRAKs, novel serine/threonine kinases related to death-associated protein kinase that trigger apoptosis. *J. Biol. Chem.*, **273**, 29066–29071.
- Schworer, C.M., Colbran, R.J. and Soderling, T.R. (1986) Reversible generation of a Ca^{2+} -independent form of Ca^{2+} (calmodulin)-dependent protein kinase II by an autophosphorylation mechanism. *J. Biol. Chem.*, **261**, 8581–8584.
- Sitkoff, D., Sharp, K.A. and Honig, B. (1994) Correlating solvation free energies and surface tensions of hydrocarbon solutes. *Biophys. Chem.*, **51**, 397–403; discussion 404–409.
- Soderling, T.R. (1999) The Ca-calmodulin-dependent protein kinase cascade. *Trends Biochem. Sci.*, **24**, 232–236.
- Steller, H. (1995) Mechanisms and genes of cellular suicide. *Science*, **267**, 1445–1449.
- Tokui, T., Ando, S. and Ikebe, M. (1995) Autophosphorylation of smooth muscle myosin light chain kinase at its regulatory domain. *Biochemistry*, **34**, 5173–5179.
- Watanabe, S., Okuno, S., Kitani, T. and Fujisawa, H. (1996) Inactivation of calmodulin-dependent protein kinase IV by autophosphorylation of serine 332 within the putative calmodulin-binding domain. *J. Biol. Chem.*, **271**, 6903–6910.
- Yang, E. and Schulman, H. (1999) Structural examination of autoregulation of multifunctional calcium/calmodulin-dependent protein kinase II. *J. Biol. Chem.*, **274**, 26199–26208.

Received May 24, 2000; revised and accepted January 2, 2001